Toward a Midlatitude Ocean Frequency–Wavenumber Spectral Density and Trend Determination

CARL WUNSCH

Department of Earth, Atmospheric and Planetary Sciences, Massachusetts Institute of Technology, Cambridge, Massachusetts

(Manuscript received 1 October 2009, in final form 20 May 2010)

ABSTRACT

The time- and space-scale descriptive power of two-dimensional Fourier analysis is exploited to reanalyze the behavior of midlatitude variability as seen in altimetric data. These data are used to construct a purely empirical and analytical frequency–zonal wavenumber spectrum of ocean variability for periods between about 20 days and 15 yr and on spatial scales of about 200–10 000 km. The spectrum is dominated by motions along a ''nondispersive'' line, which is a robust feature of the data but for whose prominence a complete theoretical explanation is not available. The estimated spectrum also contains significant energy at all frequencies and wavenumbers in this range, including eastward-propagating motions, which are likely some combination of nonlinear spectral cascades, wave propagation, and wind-forced motions. The spectrum can be used to calculate statistical expectations of spatial average sea level and transport variations. However, because the statistics of trend determination in quantities such as sea level and volume transports depend directly upon the spectral limit of the frequency approaching zero, the appropriate significance calculations remain beyond reach, because low-frequency variability is indistinguishable from trends already present in the data.

1. Introduction

Attention to oceanic variability has tended to focus on two particular, if disparate, phenomena: 1) the intense mesoscale eddy field with nominal time scales of months and spatial scales (here defined as wavelengths) of hundreds of kilometers[1] and 2) long period trends of decadal and longer time durations and (usually) of basin to global scale. Zang and Wunsch (2001, hereafter ZW2001) attempted a partial synthesis of variability that was, because of the available data, largely confined to the first phenomenon and in the Northern Hemisphere. Discussions of the second phenomenon have tended to focus on multidecadal heat and salt content changes as determined from hydrography (see the summary in Bindoff et al. 2007) and the related shifts in sea level (e.g., Cazenave and Nerem 2004). Despite the disparities of time and space scales, it is not ultimately possible, for a number of reasons, to discuss these changes separately. Of fundamental importance, one requires an accurate estimate of the nature of the background variability before significance levels can be assigned to any apparent trend. Furthermore, as climate models begin to resolve the eddy field, the question of whether they are doing so realistically in terms of basic statistics of frequency and wavenumber will loom very large. Apart from some ad hoc studies, it is difficult to describe the behavior of ocean variability between about one cycle per year and the longest periods of interest, where apparent trends are displayed. In particular, the spectral structure for length scales longer than a few hundred kilometers, on time scales exceeding a few months, is essentially unknown.

In a purely formal sense, the problem of determining the significance of apparent trends in one-dimensional stochastic data reduces to that of characterizing the behavior of the frequency power density $\Phi_s(s)$ in the limit as $s \rightarrow 0$. Smith (1993), Beran (1994), Overland et al. (2006), Vyushin and Kushner (2009), and others have discussed ''long memory'' processes in which the behavior for small s is sufficiently ''red'' that the temporal

[1] The dominant eddy field corresponds to the atmospheric synoptic scale, not the mesoscale, but it is too late to change the label.

Corresponding author address: Carl Wunsch, Massachusetts Institute of Technology, Room 54-1054, Department of Earth, Atmospheric and Planetary Sciences, 77 Massachusetts Avenue, Cambridge, MA 02139.
E-mail: cwunsch@mit.edu

DOI: 10.1175/2010JPO4376.1

covariances decay algebraically rather than exponentially as in more conventional processes. This behavior greatly reduces the number of degrees of freedom in trend estimation, and its existence would be very troubling for climate change detection. The word ''formal'' is thus used here, because in practice the behavior at the limit is both unknown and indeterminate: all real records being of finite duration and no physical system exists for infinite time. As durations increase, the characterization of real records as either stochastic or deterministic also ceases to have meaning. At best, one can try to characterize a system over time scales for which observations exist and to understand the implications should that behavior continue to be appropriate as arbitrarily longer time scales are addressed.

In this paper, some of these issues are made concrete by taking a small step toward deducing the behavior of some elements of the ocean circulation using altimetric and tide gauge records as the primary vehicle so as to frame the discussion that needs to take place for understanding trends. The altimetric record is the present focus, because it is the only one in existence exceeding a decade in length that is also continuous, near global, and—through its role as the surface pressure—representative of large-scale interior dynamics. At least three ways to use these data exist: the raw, along-track observations (for a general description of altimeter data, see Fu and Cazenave 2000), the sea surface height (SSH) derived from a GCM constrained through least squares to the raw along-track data (as in Wunsch and Heimbach 2007); and the altimetric data as gridded through the Ocean Topography Experiment (TOPEX)/Poseidon and *Jason-1* projects (Le Traon et al. 1998). The effects of gridding are not negligible but are also not of zero-order importance here; therefore, for convenience, we use that product.

In practice, as will be seen, discussion reduces to understanding the frequency–wavenumber character of oceanic variability. Because the climate system has an endless array of memory time scales—seconds to 10 000 yr in the ocean, days to 100 000 yr in the land glaciers, and arbitrarily long time scales in the biota (albedo, etc.)—the instrumental record of change can hardly be expected to depict more than a minuscule fragment of the ongoing temporal changes, whose long memory may be completely conventional.

2. The North Pacific

Basic description of altimetric data

The latitude band (see chart in Fig. 1) 20°–40.75°N spanning the width of the Pacific Ocean is used to establish the basic ideas. The analysis uses the 7-day average gridded product provided by the Archiving, Validation, and Interpretation of Satellite Oceanographic data (AVISO) project (as described by Le Traon et al. 1998), which, because it is heavily manipulated, should not be confused with the raw data. In particular, spatial scales below about 300 km have been suppressed by the gridding procedure. This region was chosen arbitrarily as likely being typical of subtropical gyres (see Zang and Wunsch 1999). Figure 2 shows four weekly estimates of the topographic anomaly in the gridded dataset. It is evident that there is strong persistence from week to week with subtle changes between weeks.

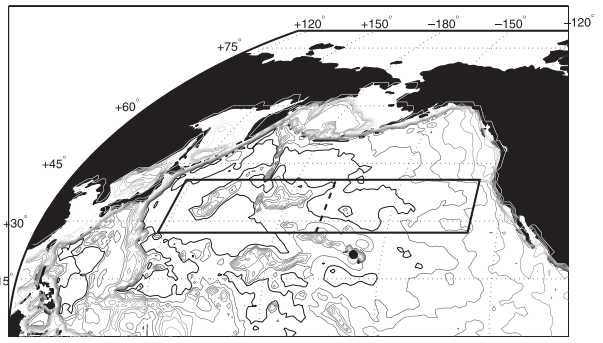

FIG. 1. Region used to study sea level and transport variability. Only the eastern half of the box (east of dashed line) is used for some of the spectral calculations to avoid the very energetic Kuroshio and Kuroshio extension region. The Hawaiian arc, the location of the Honolulu gauge (black dot), is visible just to the south of the box. The box was purposely located to avoid that major topographic interruption.

Figure 3 shows the logarithm of net temporal variance as a function of position. The three order of magnitude spatial nonstationarity in the variance renders very incomplete any simple spectral description of its behavior. (Such a description is still valid; however, unlike the case for spatially and temporally stationary fields, the ordinary spectral density is only the first term in an infinite series of higher-order spectral moments required for a complete representation.)

Sea surface height variability at any given point (here representing small regions of approximately 300-km diameter as a result of the mapping algorithm) and the areal average have distinct flavors. In what follows, the annual cycle has been left present because it is here quite weak and has been much studied (e.g., Vinogradov et al. 2008).

The spatial structure of the trends is shown in Fig. 4, which also shows some of the difficulties. The largest values exceed 30 cm yr^{-1}, but most are smaller than 10 cm yr^{-1}. On average, the trend here is positive, but it is clearly a small residual of positive and negative changes (this region is that of the Kuroshio extension and on the west is one of the noisiest parts of the ocean).

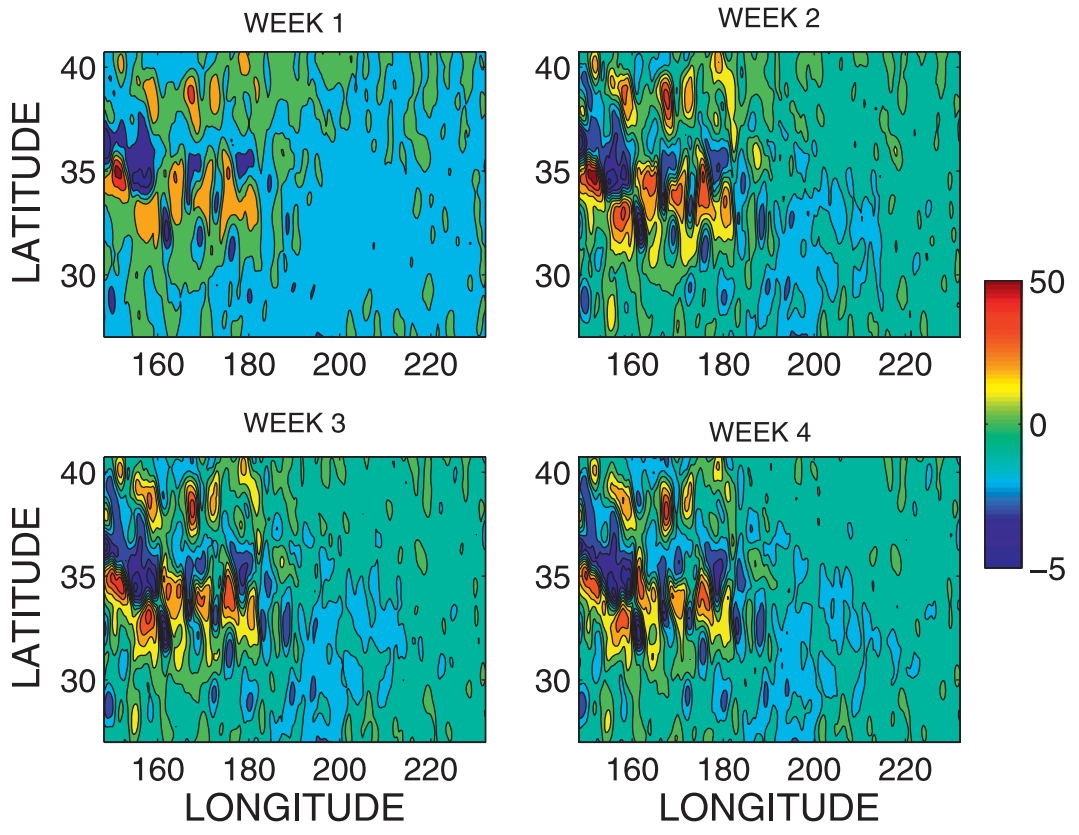

FIG. 2. Sea surface anomaly (cm s^{-1}) at weekly intervals showing the degree of variability present. Week 1 starts on 14 Oct 1992.

Estimates of the near-global trends can be seen in Cazenave and Nerem (2004) and Wunsch et al. (2007), among others.

3. Periods to 15 yr

Consider the k–s (circular wavenumber and frequency) power density estimate $\Phi(k, s)$ of surface elevation η shown in Fig. 5 from altimetric data (Wunsch 2009) in the eastern region of the North Pacific box (a similar set of results from the South Pacific Ocean can be seen in Maharaj et al. 2007). Its integrals are the frequency and wavenumber spectra,

$$\Phi_k(k) = \int_0^{s_{\max}} \Phi(k,s)\, ds, \quad \Phi_s(s) = \int_{-k_{\max}}^{k_{\max}} \Phi(k,s)\, dk, \qquad (1)$$

where the limits are determined by the sampling properties of the gridded values, and they are shown in Fig. 6. These diagrams were described by Wunsch (2009). Here, note particularly that much of the energy lies along the "nondispersive" line in wavenumber–frequency space. Chelton et al. (2007) and many other authors have focused on these motions. A significant fraction of the energy exists, however, at large distances from this line, including that of eastward-going motions (20% of the total is eastward, 70% is westward, and 9% is indistinguishable from standing wave energy). The nondispersive line is nearly tangent to the first baroclinic mode dispersion curve (shown in the figure) near zero (k, s) and intersects the barotropic dispersion curve at large (k, s). This behavior appears to be typical of much of the ocean, but with high latitudes, including the Southern Ocean, being distinctly different (not shown here).

An estimate of the corresponding meridional wavenumber–frequency spectrum is shown in Wunsch

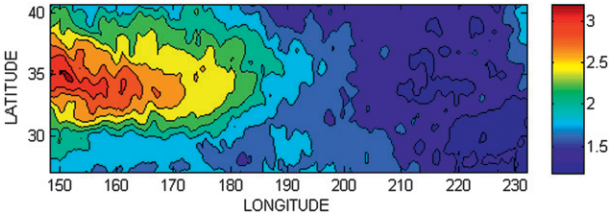

FIG. 3. Base 10 logarithm of the sea surface variance (cm^2) showing the great spatial inhomogeneity of the field. This chart visually is only a little different when the annual cycle is removed.

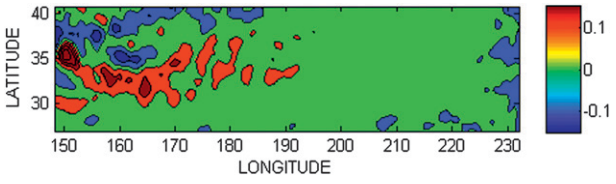

FIG. 4. The trend, in meters per year in the region. In general, the trend is much less than the standard deviation.

(2009) with a predominance of long-meridional-scale energy and is not further considered here. [Glazman and Weichman (2005) discuss the general topic; accounting for a meridional wavenumber result expressed in radians, their inferred meridional wavelengths are consistent with those found here but are not displayed.] Suggestions exist that zonal jet-like features are important in the ocean circulation (e.g., Maximenko et al. 2008, and references therein); if present in the altimetry at this location, however, they are relatively very weak in the time-dependent components. (Geoid accuracy is insufficient on those scales to discuss the time mean.) Ultimately, the results here need to be extended to include the meridional structure (C. Wortham 2010, personal communication).

It is not the intention in this paper to produce a global discussion but to provide a framework for it. Figure 7 displays the logarithmic frequency–zonal wavenumber spectrum for the considerably higher latitude of 41°N, the northern edge of the study box. A residual of the nondispersive line is visible, lying along a much less steep straight line. Consistent with inferences of Tulloch et al. (2009), the dominance of the excess energy along the nondispersive line is reduced, with a corresponding relative increase in the energy of the eastward-going motions and much energy close to $k = 0$. At the northern edge of the box, the relative energies are nearly equally divided between eastward- and westward-going motions, and the ZW2001 representation becomes more accurate.

A reviewer of this paper insists that adequate theory exists to explain the structure of Fig. 5; thus, we briefly digress to summarize some of the issues, which are treated at greater length by Ferrari and Wunsch (2010, hereafter FW2010; see also Vallis 2006, etc.). Beginning with Chelton and Schlax (1996), the published focus has been on the apparent phase velocity of altimetric disturbances, often determined through a Radon transform. This approach calculates straight-line integrals through the longitude–time fields, seeking the maximum value corresponding to the dominant phase velocity. It lumps together all wavenumbers irrespective of frequency and thus isolates the existence of the nondispersive line as the dominating feature of the data at midlatitudes and low latitudes.

Theoretical explanations for the makeup and structure of the overall wavenumber and frequency–wavenumber spectra fall into a small number of categories: 1) wave theories, in which the motions are dominantly free, with a physics ranging from the "basic textbook theory" (BTT) of a flat-bottom, linear, resting, etc., ocean to their modification by variable background flows, stratification, topography, etc.; 2) instability theories, where the variability results from the breakdown of mean currents and is described by waves with properties of the most unstable modes, possibly equilibrated but overlapping the physics contained in 1); 3) forced wave theories,

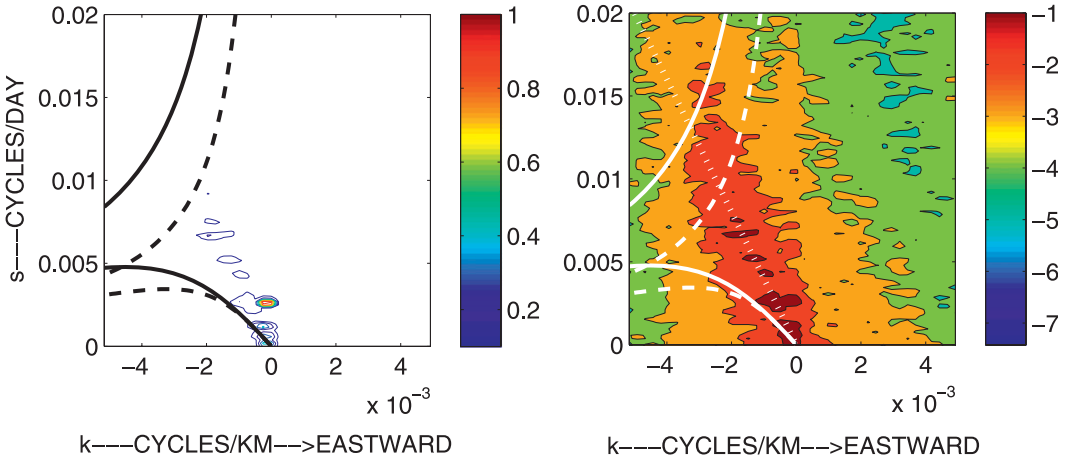

FIG. 5. Normalized frequency–wavenumber spectrum as estimated for the eastern subregion in Fig. 1 (from Wunsch 2009) along 27°N. (left) The power linearly and (right) its logarithm. Normalization renders the maximum value as 1 so that only the shape is significant here. Dashed lines show the linear Rossby wave dispersion relationship in the barotropic and first baroclinic modes, with the meridional wavenumber $l = 0$, and the dashed–dotted lines assume $l = k$ for unit aspect ratio.

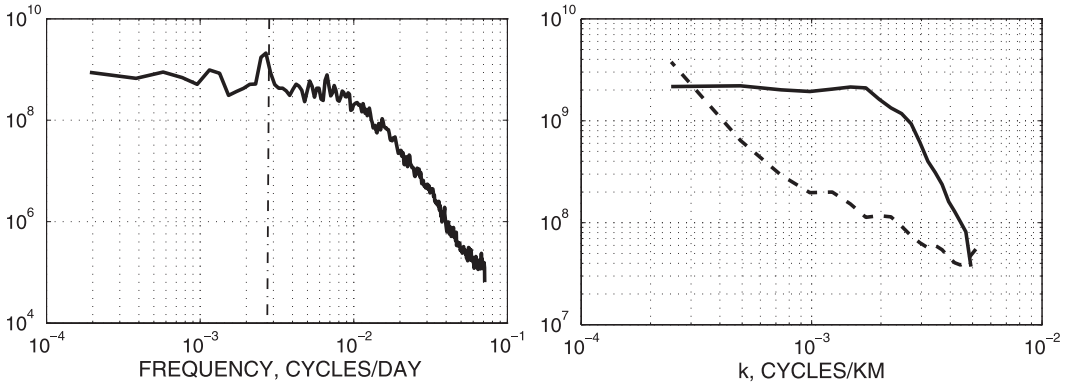

FIG. 6. (left) Frequency $\Phi_s(s)$ and (right) zonal wavenumber $\Phi_k(k)$ spectra of η for the eastern part of the study region. Wavenumber spectra are shown as westward-going (solid) and eastward-going (dashed) energy. Vertical dashed–dotted line denotes the annual cycle, which is only a small fraction of the total energy and is dominated by the lowest wavenumbers (see Fig. 5), indistinguishable here from $k = 0$. Approximate 95% confidence limits can be estimated as the degree of high frequency or wavenumber variability about a smooth curve and are quite small (from Wunsch 2009). The one-dimensional spectra are not normalized.

encompassing both stable and unstable background flows. As wave theories, all three of these theories can produce dispersion relationships between k (and/or l) and s, although in the forced case the k–s space is filled out by the imposed forcing spectrum subject to full or near-resonant amplifications. Another category is 4) turbulence theories that result in a disordered field, with no dispersion relationship available. The ultimate energy sources can be either or both of forced or unstable motions. Theory predicts only the k spectra, but Eulerian frequency spectra can sometimes be inferred through Taylor's hypothesis $s = Uk$, where U is either a large-scale advective flow or an RMS velocity of the energy containing eddies. Further theory predicts the emergence of wave physics at meridional scales larger than the Rhines (1977) $L_R \propto (U/\beta)^{1/2}$, because turbulence is arrested at those scales (β is the conventional meridional derivative of the Coriolis parameter). These elements overlap and interact. For example, Isachsen et al. (2007) show how instability of the waves in 1) can drive energy away from any dispersion curve.

A full review of these various theories and their relationship to the empirical spectra would require much more space than is available here. Suffice it to say that the predominant motions present do not have an obvious relationship to 1), except at the very lowest observable frequencies, where they are indistinguishable from the linear dispersion curves. Both the Taylor hypothesis and turbulent flows subject to β effects involve parameters usually labeled U. Taylor originally defined U as a large-scale mean velocity advecting isotropic turbulence past fixed sensors (see, e.g., Hinze 1975), although it has been reinterpreted in the Rhines (1977) sense as an eddy RMS. In the present case, it is difficult to see why, in either case, U should have a latitudinal dependence producing the nondispersive line slope of βR_d^2 or how the RMS advecting flow could be so remarkably stable that the slope is maintained so sharply for 16 yr. None of the spectra examined here shows a wavenumber gap permitting an easy selection of the transition between energy- and enstrophy-dominant scales, nor to my knowledge does the theory permit an explicit calculation of the structure seen in Fig. 5. FW2010 concluded that wind-forced motions describe a significant fraction of the observed motions not on the nondispersive line, but not necessarily a majority of it.

Included in the wave theories is the literature rationalizing the "too fast" phase velocity first pointed out by

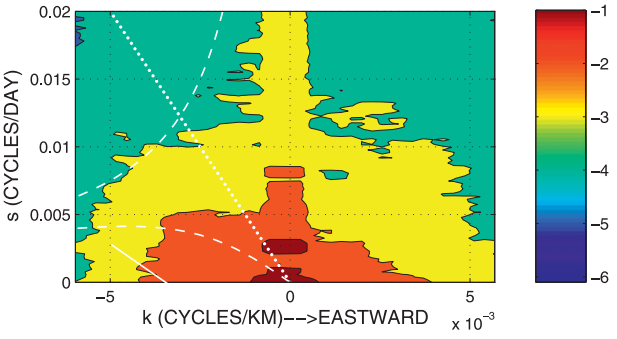

FIG. 7. The logarithm of the energy density, as in Fig. 5, but at 41°N. The thin white line is the new tangent to the first baroclinic mode at $s = k = 0$, and the dotted white line is the tangent line of Fig. 5. At this higher latitude, the tangent line is much shallower. Notice that the energy lying along the nondispersive line is reduced, with a noticeable corresponding growth near $k = 0$ at all frequencies. Dashed white lines are the linear dispersion curves for the barotropic and first baroclinic modes with $l = 0$.

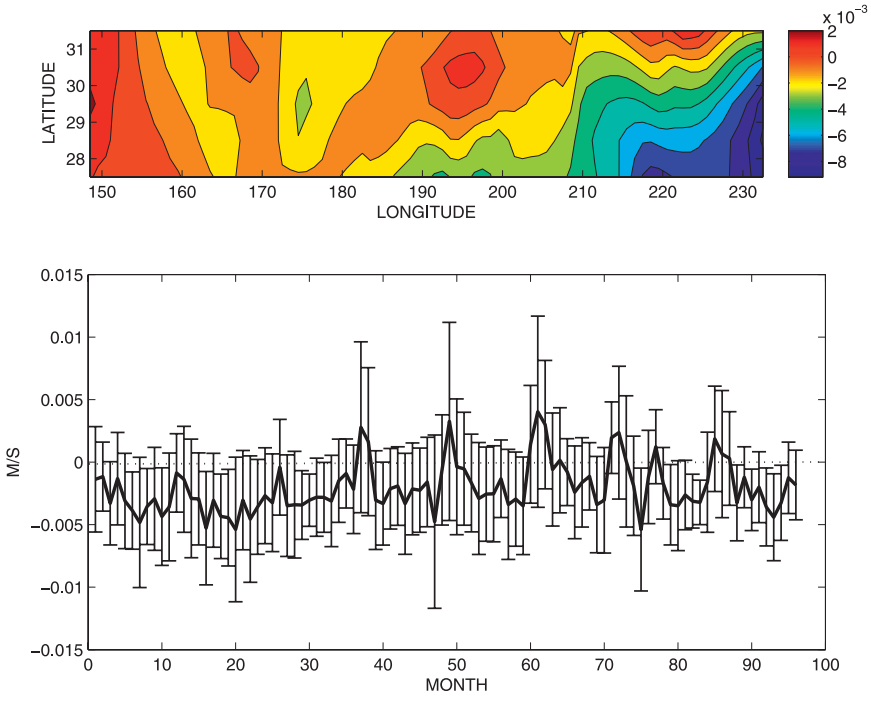

FIG. 8. (top) Contours in m s^{-1} of the time average zonal flow u over 16 yr at each point in the latitude–longitude range shown from ECCO-GODAE solution v3.73. (bottom) The spatial average velocity over the latitude band of (top), but only the eastern half of the region, along with its spatial standard deviation.

Chelton and Schlax (1996). Maharaj et al. (2007) show that the mean potential vorticity theory of Killworth and Blundell (2003b) describes much of the motion along the low-frequency end of the nondispersive line in the South Pacific but not the energy located elsewhere in s–k space. Again, why the nondispersive line should emerge with the slope βR_d^2, noted above, is not so clear. Alternative hypotheses also exist, particularly those related to the influence of bottom topography (Tailleux and McWilliams 2001; Killworth and Blundell 2003a), whose tendency to reduce the abyssal velocities can produce coupled modes with faster phase velocities. This latter mechanism will be touched on later, because it has testable consequences for mooring data.

a. Behavior of U

The existence of the variable U in the turbulence theories suggests the utility of a brief examination of the temporal and spatial structure of the large-scale flows. Consider, as an example, the large-scale flow field in the boxed region as inferred from the Estimating the Circulation and Climate of the Ocean–Global Ocean Data Assimilation Experiment (ECCO-GODAE) solution v3.73 discussed by Wunsch and Heimbach (2009). This estimate, based on a 1° horizontal resolution GCM, represents a least squares fit to a very large dataset coincident with the altimetric record used here, including not only the altimetry but also hydrography, etc. No eddies are present with this resolution, and in the open ocean the resulting time-varying estimate can be thought of as a field in thermal wind balance, within error bars, of all of the data, thus reflecting the gradients on subbasin and larger scales. To keep the discussion from proliferating unduly, we use the water-column average monthly-mean zonal flows, setting aside the difficult question of the vertical structure of U. This choice is made because, as discussed below, current meter mooring data are interpreted here as implying a linear low mode (the barotropic and lowest baroclinic modes) structure, one which could not be maintained in a strongly sheared, time-varying, background flow. Hypotheses depending on the depth of integration could be explored but are not taken up here.

The latitude range was restricted to 27.5°–31.5°N. Figure 8 shows the monthly-mean U and its spatial standard deviation over the strip as well as the time average of U showing the spatial structure. In general, the time average $U \ll \beta R_2^2$, the approximate slope of the nondispersive line, but its variability is sufficiently great that it could broaden the dispersion curve. Kinetic energy in the ocean is 95%–99% bound up in the variability (e.g.,

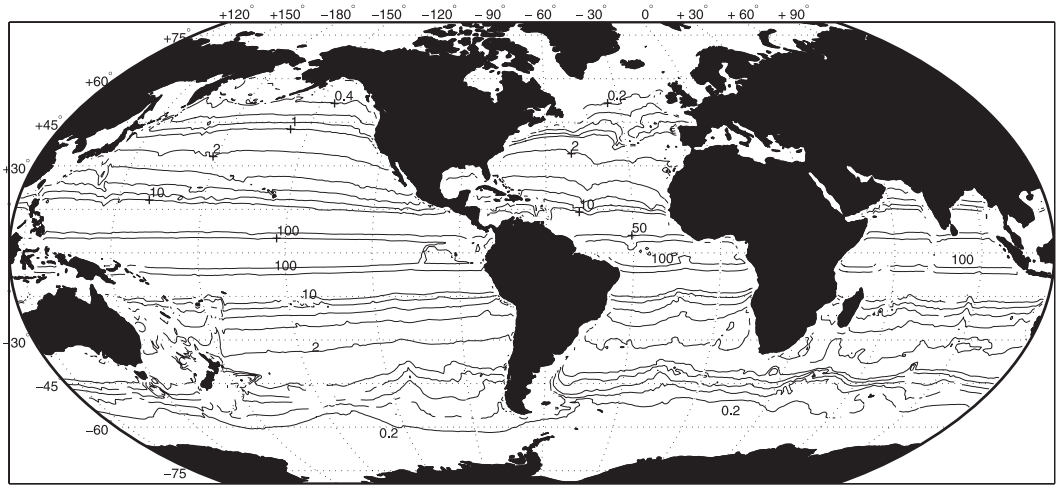

FIG. 9. Slope of the first baroclinic mode dispersion relationship as $s \to 0$ as a function of position. Evaluated from Chelton et al. (1998). Values are in kilometers per day. The dispersion relationship is modified near the equator, from the equatorial β plane, and values are not shown.

Ferrari and Wunsch 2009). All this simply says that the ocean appears noisy out to the longest records that we have and that choice of where to separate large and mesoscales is an arbitrary one, precluding a simple estimate of U in any of its definitions.[2]

b. An analytical curve fit

Can one find an analytical form sufficiently accurate to use in calculating temperature or transport variations and trends? Among the many possibilities are the one the same referee insists is the ''correct'' one,

$$\Phi(k, s) = \frac{A(\phi, \lambda)}{(s + k\beta R_d^2)^2 + a_1^2}, \tag{2}$$

where a_1 is a constant, which emerges from the linear damped-resonance model, for example, of Frankignoul et al. (1997). This form was one of the first tried (not shown) but was rejected because it gave a poor fit, both in not exhibiting the narrowness and large amplitude of the nondispersive line energy and because it failed to adequately describe the significant amounts of energy lying far from that line. Consider, instead, as a starting point,

$$\Phi(k, s) = A(\phi, \lambda)\left\{\mathrm{sech}^4\left(\frac{\beta R_d^2 k + s}{0.008}\right)\exp[-(100s)^2] + \frac{0.01}{a_1 + a_4 k^4 + \delta_1 s^2}\right\}, \quad 0 \le s \le 1/7d, \quad -1/100 \le k \le 1/100\,\mathrm{km}$$
$$\beta R_d^2 = 4\,\mathrm{km/d}, \quad a_4 = (200\,\mathrm{km})^4, \quad a_1 = 0.01, \quad \delta_1 = (14\,\mathrm{day})^2, \tag{3}$$

where the sech^4 produces the excess energy along the nondispersive line in Fig. 5 and the second term accounts for the broad continuum away from that line. The sech^4 term was introduced to represent the exponential decline in energy away from the nondispersive line. The only physically based parameter is βR_d^2, and a crude accounting for latitudinal changes within the subtropics can be obtained by permitting $\beta(\phi)R_d(\phi, \lambda)^2$ to be a slowly varying function of position (latitude ϕ and longitude λ); $A(\phi, \lambda)$ is intended to be a slowly changing function of position, as in the ZW2001 energy amplitude factor. Figure 9 shows how βR_d^2 varies with position, primarily with β. At high latitudes, the maximum phase velocities are so slow that linear physics are unlikely to apply (note 1 km day$^{-1} \approx 1$ cm s^{-1}).

This form represents the nondispersive motions as additive to a background continuum, displaying both wave-like and turbulence-like characteristics. The result is purely empirical and no claim is made that is correct, merely that it provides a reasonably efficient description

[2] One might argue that U should be determined by the eddy field that has been suppressed here by use of a 1° horizontal resolution model. However, eddy-permitting models (e.g., Mazloff et al. 2010) show no recognizable dividing point between the eddy field and larger-scale flow, and no such model has yet been run constrained to be consistent with the global datasets. In any event, it is not so easy to test such models for realism. Any field $\tilde{U}$ derived from the eddy field will show a stochastic behavior that would need to be tested.

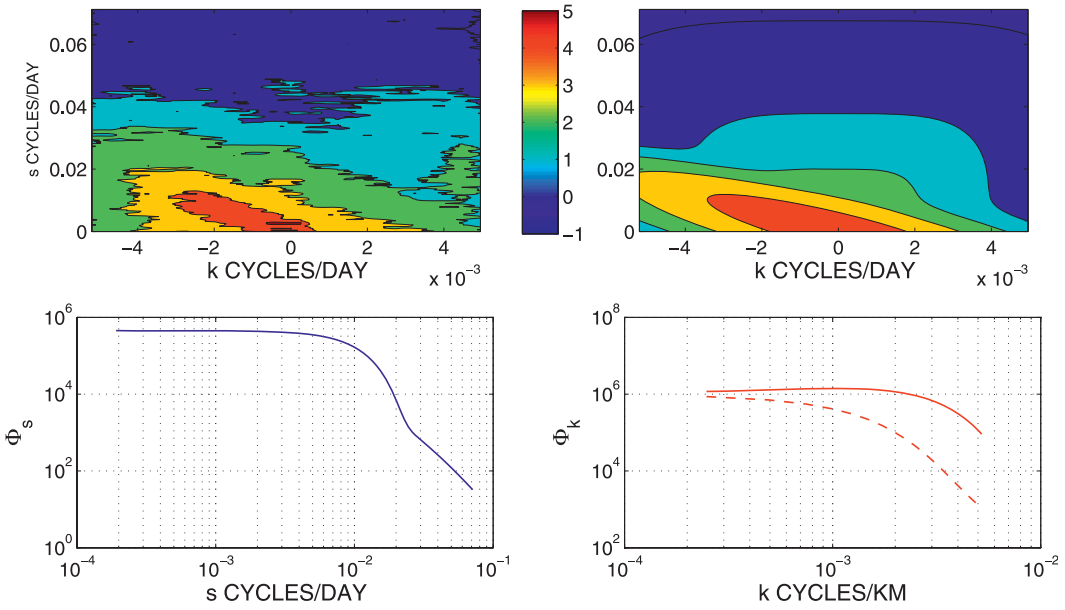

FIG. 10. (top) (left) The logarithmic spectrum as in Fig. 5 and (right) the suggested analytical form in Eq. (3). (bottom) The summed out (left) $\Phi_s(s)$ and (right) $\Phi_k(k)$. The values are normalized so that the power sums to 1, not as in Fig. 5.

of the estimated spectrum. Figure 10 shows that the analytic form does a reasonable job. In comparison to $\Phi_k(k)$, the form produces relatively too much eastward-going motion and an inadequate roll off in wavenumber. It is important to keep in mind, however, that the high wavenumber behavior, beyond about 1/200 km, of the altimetric data is essentially unknown. The high-frequency limit $s_m = 1/14$ day corresponds to the 7-day gridding interval AVISO product. Note that the Garrett and Munk (1972) internal wave spectrum contains energy at 100 km and shorter, and there is as yet no way of separating internal wave energy from that of the geostrophically balanced flows (see, in particular, Katz 1975). The conspicuous appearance of internal tides in altimetric data shows emphatically that internal waves more generally will be present in altimetric data. A full oceanic frequency–wavenumber spectrum eventually must reflect the contribution from internal waves, balanced motions, and other ageostrophic energy. Because of the very large spatial variation in oceanic kinetic energies, A is chosen to impose,

$$\int^{\infty}\int_{-\infty} \Phi(k,s)\, dk\, ds = 1,$$

approximately, so that a local altimetric variance can be introduced as a multiplier to produce any regional energy level. As $s \to 0$, both $\Phi(k, s)$ and $\Phi_s(s)$ are independent of s, rendering the frequency spectrum as white noise. That inference is reexamined below.

As compared to ZW2001 and as used in Wunsch (2009), the form in Eq. (3) is nonseparable in k, s, which leads to greater analytical difficulties. A multitude of motions are being depicted, including free modes, meteorologically forced motions reflecting atmospheric structures, the end products of turbulent cascades, ageostrophic motions having a surface expression, advection of near-frozen features, and instrumental noise, all superposed and sometimes interacting. A marginally better fit is obtained by retaining terms in k, k^2, etc., but they are probably not now worth the extra complexity.

The term in $\beta R_d^2 k + s$ reflects the inference that the nondispersive line is approximately tangent to the first-mode baroclinic Rossby wave dispersion curve as $(k, s) \to 0$ (see Wunsch 2009), which is suggested by the way the slope changes with latitude (Fig. 9). In practice, at best, one can say only that the tangency is not inconsistent with the data, albeit the estimated values of R_d are necessarily noisy and the utility of a resting ocean hypothesis is doubtful for small s.

Both the estimate in Fig. 5 and the analytic expression, Eq. (3), contain a great deal of structure, implying that a choice of the various constants in the analytic expression will produce varying accuracies over the k–s plane. At this stage, it is not completely clear what the most significant elements are. To proceed, note (e.g., Vanmarcke 1983) that many of the physically important properties of a Gaussian random field depend only on the spectral moments. Thus define,

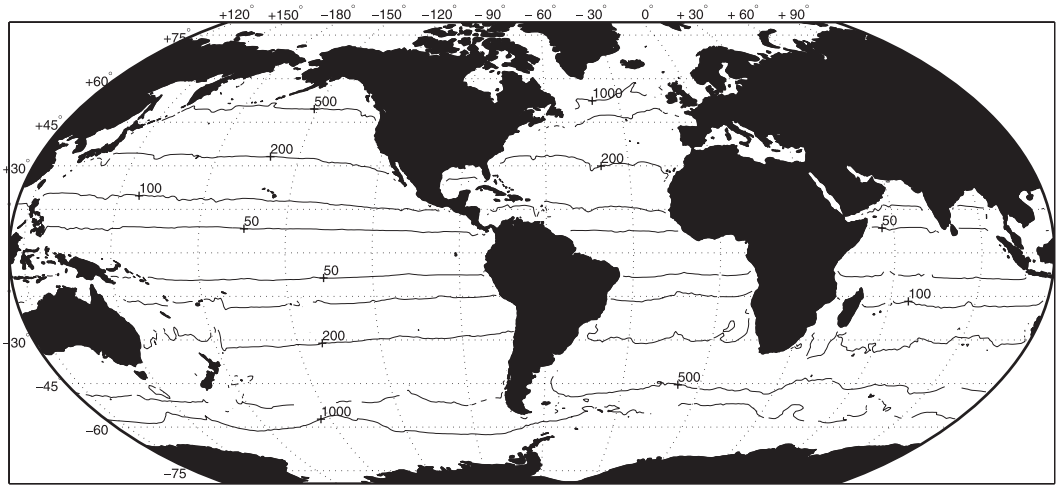

FIG. 11. Estimate of the shortest period (days) possible in the first baroclinic Rossby wave, computed from βR_1, where R_1 was estimated by Chelton et al. (1998). Values near the equator must be computed from a different dispersion relationship and are not shown here.

$$\langle s^q \rangle = \int_0^{s_m} s^q \Phi_s(s)\, ds \Big/ \int_0^{s_m} \Phi_s(s)\, ds,$$

$$\langle k_w^q \rangle = \int_0^{k_m} k^q \Phi_k(k)\, dk \Big/ \int_0^{k_m} \Phi_k(k)\, dk,$$

$$\langle k_e^q \rangle = \int_{-k_m}^{0} k^q \Phi_k(k)\, dk \Big/ \int_{-k_m}^{0} \Phi_k(k)\, dk,$$

where q is an integer. From the data, $1/\langle s \rangle = 164$ day, $1/\sqrt{\langle s^2 \rangle} = 121$ day, $1/\langle k_w \rangle = 696$ km, $1/\sqrt{\langle k_w^2 \rangle} = 579$ km, $1/\langle k_e \rangle = 1710$ km, and $-1/\sqrt{\langle k_e^2 \rangle} = -1/905$ km. These values are independent of A. That the westward-going moments have shorter wavelengths than the eastward-going ones is consistent with the excess energy along the nondispersive line. One now has to choose the constants in Eq. (3) so that these moments are approximately reproduced. In comparison, the values obtained are, 177 day, 138 day, 573 km, 471 km, 1128 km, and 899 km, which are considered sufficiently close to the empirical ones to proceed (a formal fitting procedure could be employed). These values conveniently characterize the space and time scales of the variability, albeit with much loss of detail.

Because the frequency tends toward $^1/_{15}$ yr, the asymptotic spectral values are not trustworthy. Among other reasons, any trend present in the data will influence the spectral shape (see the appendix for a brief discussion of the trend fitting problem). The spatial structure of the trends shown in Fig. 4 demonstrates some of the difficulties.

In the BTT theory (Longuet-Higgins 1965), the highest frequency possible in a linear, first-mode Rossby wave is $s = \beta R_1/4\pi$, which diminishes rapidly with latitude. The slope of the dispersion curve (the group velocity) as $s \to 0$, diminishes as βR_1^2. Thus, as the latitude increases, the domain of the first-mode Rossby wave becomes very small, higher modes having yet longer periods, and the linear, free-wave dynamics are decreasingly relevant (see Fig. 11). A high-latitude theory is thus potentially, in one respect, simpler than a midlatitude one in eliminating the wave mechanisms present in the physical process list above.

c. The low frequencies and wave numbers

We now turn specifically to the spectral behavior with frequency and the behavior at periods longer than are accessible from the altimetric record. Mitchell (1976), Kutzbach (1978), Huybers and Curry (2006), and others have provided discussions of the spectrum of climate extending back into the remote past in a subject notable for its extremely scarce data.

As a guide, we start with the 103-yr record available from the Honolulu, Hawaii, tide gauge record (latitude 21.3°N just to the south of the altimetric box; taken from the Web site of the Permanent Service for Mean Sea Level, Liverpool, United Kingdom), plotted in Fig. 12. This record is discussed in detail by Colosi and Munk (2006); although the presence of the Hawaiian island arc raises questions about its representativeness of the open ocean, it at least provides an example of the problems faced in describing low-frequency behavior of the sea surface height at time scales much longer than obtainable from the altimetric duration. Figure 12 shows the spectral density estimate of the record calculated in two distinct ways, both for the original and detrended (trend

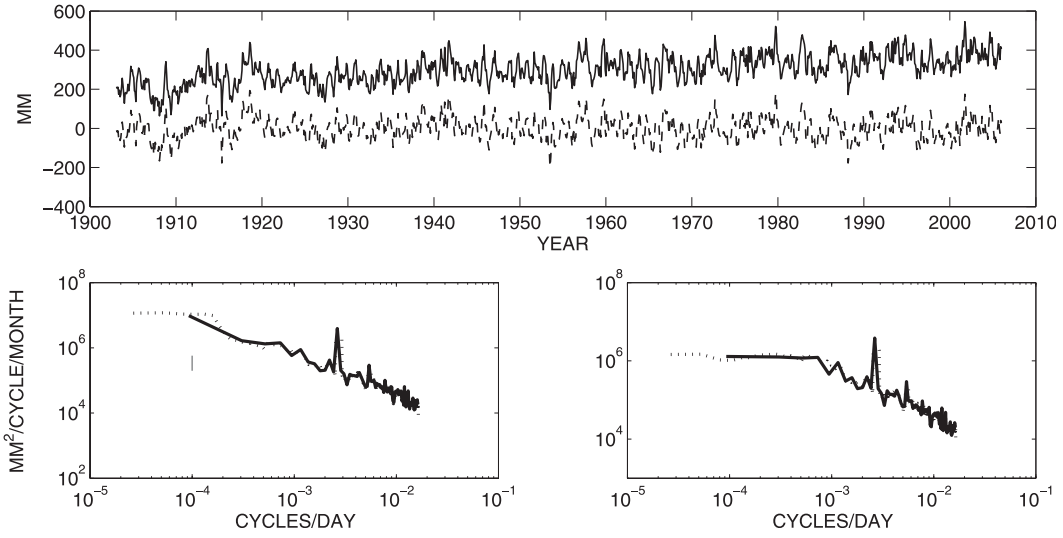

FIG. 12. (top) The monthly-mean 103-yr Honolulu tide gauge record (from the Permanent Service for Mean Sea Level), before and after trend removal [see Colosi and Munk (2006) for a detailed discussion of this record]. (left) Two power density spectral estimates are shown before trend removal. One estimate is from a Daniell window applied to a periodogram (using eight frequency bands; solid line), and the second is a multitaper spectral estimate (Percival and Walden 1993; dotted line). Approximate 95% confidence interval is for the latter. A power law of $s^{-1.1}$ is a best fit to the multitaper estimate in the frequency band corresponding to periods between about 500 and 55 days. (right) At the lowest frequencies, removal of the trends shifts the spectral shape from weakly red to nearly white.

of 1.5 ± 0.05 mm yr^{-1}) records.[3] The first method is based on a Daniell-window smoothed periodogram, and the second is the multitaper method (see, e.g., Percival and Walden 1993). Because the multitaper method is biased at low frequencies (McCoy et al. 1998), the periodogram method provides the better estimates for small s. The major issue concerns the conventional trend removal, which in all cases shown converts the somewhat red spectrum at low frequencies into one that is reasonably described as white noise. Is the trend the secular one reflective of the extended deglaciation discussed below, is it another low frequency fluctuation that will ultimately reverse, or is it an artifact of changing observational technologies and instrument positions? For present purposes, we explicitly assume that the trend is truly secular, defined as extending far beyond the record length, and will take as a starting point the assumption that, at periods beyond about a 5-yr period, the spectral density of sea surface height is white noise. [Sturges and Hong (1995), suggested a drop in the spectral density at Bermuda for periods longer than about 8 yr, but they were extrapolating beyond the region of conventional spectral estimation.]

The issue of the asymptotic value, $s \to 0$, of the spectrum is difficult. Huybers and Curry (2006) patched together various proxy data that can at least crudely be interpreted as large-regional-scale temperatures extending back beyond 100 000 yr. If taken literally (proxy records are not simple to interpret), a power law slope $s^{-1/2}$ would be representative out to about 100-yr period, becoming much steeper than that at longer periods to about 100 000 yr (where there is an energy excess). Their proxy spectra appear to flatten beyond 100 000 yr, rendering the energy in the physical process as finite. However, on the very longest time scales imaginable (gigayears), one has the formation of the ocean, which is not obviously stochastic. Evidently, very different physical regimes exist as time scales change, and any attempt to infer the limiting behavior $s \to 0$ will fail with a finite record length.

What do such results imply for the ocean? Assume that the Huybers and Curry (2006) results nominally represent atmospheric temperatures T_a. In one of the simplest of all possible models, oceanic temperatures might depend on the atmospheric ones through a rule,

$$\rho c_p V \frac{\partial T}{\partial t} = \gamma (T_a - T), \tag{5}$$

where γ is some constant, c_p is the oceanic heat capacity, and V is some relevant volume. Then the power density of ocean temperature is related to that of T_a (denoted Φ_a) as

[3] The standard error is based on the assumption of a white noise background and is thus optimistic. That the trend is best regarded as a straight line is an assumption, one that is discussed further in the appendix.

$$\Phi(s) = \frac{\gamma'^2 \Phi_a(s)}{s^2 + \gamma'^2}, \quad \gamma' = \gamma/\rho c_p V. \tag{6}$$

If $\gamma' \gg s$, $\Phi(s) \propto \Phi_a(s)$ and will have the same power law. On the other hand, if $\gamma' \ll s$, $\Phi(s) \propto \Phi_a(s)/s^{-2}$ and will be much steeper. A choice of γ is crucial. In modern ocean models, the time scales for ocean surface temperatures to be ''nudged'' toward atmospheric ones range from a few days to a month or so (see, e.g., Frankignoul et al. 1998); thus, $s^2 \ll \gamma'^2$, and $\Phi(s) \propto \Phi_a(s)$. On very long time scales, this relationship is almost surely incorrect, with the two fluids interacting in a complicated way.

However, to establish a straw man, supposing the proxy temperatures to be proportional to ocean heating, one would infer that, on time scales somewhat longer than available in the altimetry, the sea level spectrum should become a bit steeper than white noise ($\approx s^{-0.3}$) as in $\Phi_a(s)$. The simplest rationalization for the absence of evidence for this behavior is that the altimetric sea level data at periods between about 1 and 15 yr are not dominated by thermodynamic processes but are primarily a mechanical response to wind fluctuations having a near-white frequency spectrum (see, e.g., Sturges and Hong 1995; Frankignoul et al. 1997; Sturges et al. 1998). At much longer periods, presumably the thermodynamic (and freshwater exchange) response would be great enough to emerge from the wind-driven circulation backgrounds.

We here propose a straw man power density spectrum for the oceanic pressure field, one that would also approximate the sea level power density, extending out to the 100-kyr time scale of the glacial–interglacial shifts of the late Pleistocene. We suggest that, at periods of about 100 kyr and longer, the power density is white noise. The presumption then is that, at periods between about 100 kyr and 50 yr, the oceanic response is to an approximate buoyancy forcing (manifesting itself both through freshwater injection–removal and thermal transfers), interpreting the Huybers and Curry result as implying a temperature change with power density of approximately s^{-1}, thus producing an oceanic sea level change proportional to s^{-1} as Eq. (7) would suggest.

Between 50 and 15 yr, it is supposed that the sea level frequency spectrum is approximately white (as seen in Fig. 12), again forced primarily by atmospheric wind fluctuations. As $s \to 0$, Eq. (3) is constant in s, implying white noise in frequency, which is accepted as at least not inconsistent with present knowledge. Apart from what is implicit in the frequency–wavenumber spectrum itself, not much is known of the degree to which the small-scale structures persist into very low frequencies; that is, does the mesoscale have a low-frequency cutoff? To render the spectral result somewhat less abstract, Fig. 13 displays four 4-yr-mean sea surface height anomalies relative to the 9-yr mean, 1993–99, subtracted from the AVISO product (R. Ponte, 2009, personal communication). That much of the small-scale structure persists through 4-yr averages (and a 16-yr one; not shown) suggests that no such mesoscale frequency cutoff exists. These structures are not time-independent ''standing eddies'' but temporal anomalies.

The spectral energy must vanish on scales larger than the ocean basins. Beyond that, little is known, although some qualitative inferences can be made from the fragmentary observations of large-scale hydrographic variability. A considerable literature has now developed showing ''trend like'' behavior in the large-scale hydrographic fields (Roemmich and Wunsch 1984; Joyce et al. 1999; Arbic and Owens 2001; Polyakov et al. 2005; Johnson et al. 2007, and many others.) These results are plagued by poorly documented changes in observational technologies and calibrations over time, strong spatial and temporal aliasing, near-surface seasonal biases, and often the use of unjustified long-distance extrapolations of sparse results. Just as temporally intermittent sampling of noisy data can produce apparent long-term trends (see, e.g., Wunsch 2008), sparsely sampled noisy spatial fields can produce spurious large-scale shifts. On the other hand, there is no evidence in the ocean for any sort of spectral gaps, and one expects a forced, turbulent system like the ocean to vary on all time and space scales. Thus, large-scale, low-frequency oceanic variability is almost surely present, out to the long-wavelength cutoff at the oceanic basin scale of about 40 000 km.

Interpretation of published hydrographic results confronts exactly the same problems of interpretation already encountered in the altimetric–sea level datasets: is one seeing a secular trend or ''merely'' a long-term red-noise fluctuation hugely exaggerated in difficulty by the comparatively (to the sea level measurements) space and time sampling sparsity? [Bryden et al. (2003) is a rare report of apparently oscillatory behavior in long-term hydrographic data.] To account formally for the very long time, large-scale behavior, Eq. (3) is modified to

$$\Phi(k, s) = [1 - \exp(-D^2 k^2)] B(s,k) A(\phi,\lambda) \times \left[\operatorname{sech}^4(\beta(\phi) R_d(\phi,\lambda)^2 k + s)/0.008 \exp(-100 s^2) + \frac{1}{a_1 + a_4 k^4 + \delta_1 s^2} \right],$$
$$D = 8.6 \times 10^3 \text{ km}, \quad s > 0 \tag{7}$$

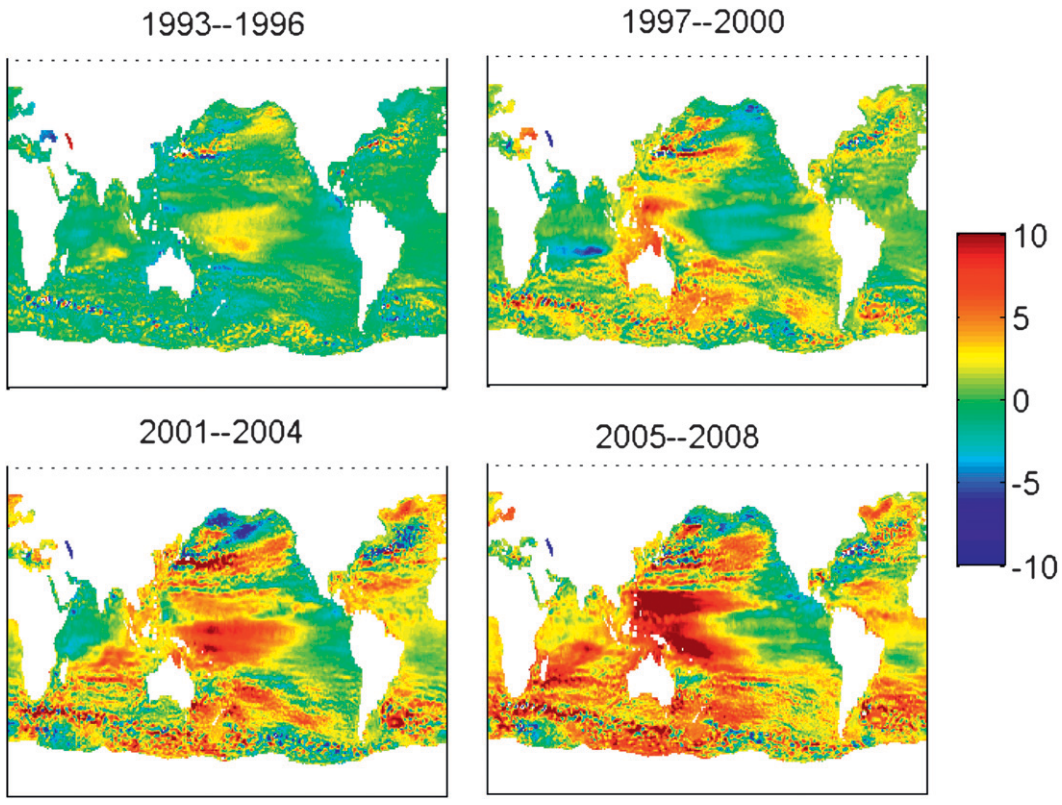

FIG. 13. A 4-yr time average of the AVISO altimetric product relative to the 9-yr mean surface. That small-scale structures are observed even after 4 yr of averaging suggests that the mesoscale can exist at all frequencies (R. Ponte 2009, personal communication) Note that the anomalies are relative to a 9-yr mean subtracted by the AVISO group and not coincident with the entire record length.

where the leading factor suppresses the energy as $1/k \rightarrow$ 40 000 km; $B(s, k)$ describes the further multiplicative modification of the frequency–wavenumber spectrum in the range $1/40\,000 \text{ km} \leq k \leq 1/20$ km, $0 < \varepsilon_1 \leq s \leq 1/15$ yr; and ε_1 is a small, unspecified number introduced to prevent the zero frequency limit from being inferred. Given the difficulties described of interpreting the low-frequency variability, at the present time, B is tentatively written as

$$B(k,s) = \frac{1}{b_1 + b_2 s},$$

with the constants unspecified. Determining its true form will be a challenging problem. The value of D brings Φ to 95% of its full value when $k = 1/5000$ km.

4. The vertical structure

Little has been said thus far about the vertical structure of the corresponding pressure fields. This problem is discussed by Wunsch (2009) and FW2010: the major difficulty is that almost everything that is known from observation is based on the mooring results in Wunsch (1997) and similar studies, which are spatially scattered and of limited duration and vertical coverage. A very rough inference is that about 50% of the water-column kinetic energy lies in the barotropic mode (a bit less in the Pacific and a bit more in the North Atlantic), and 30%–40% lies in the first baroclinic one (modes being the BTT ones defined for a flat-bottom and unforced free surface). The remaining kinetic energy lies in higher modes and observational noise. Because the relative contribution of the first baroclinic mode to the surface kinetic energy, as seen by an altimeter, is greatly amplified because of the general increase of the buoyancy frequency toward the surface, it is easy to forget the important role of the barotropic mode in the great bulk of the water column. At periods beyond about a year, there is essentially no information from observations and little prospect for any, without a dedicated observation program, rendering it difficult to test what model results exist. Altimetric data are, more generally, insensitive to high vertical mode structures or wavenumbers because of the physics of the effectively near-rigid sea surface. This strong suppression of short-wavelength

vertical structures in the movement of the sea surface is sometimes forgotten.

The BTT modes used in Wunsch (1997) are a complete set for representing (u, v)—the solution to a Sturm–Liouville problem—but they would become an inefficient representation for motions confined at or near the sea surface and/or those being forced there by w. Philander (1978) reviews the structure of motions forced at the sea surface and a nonlinear generalization has been given under the title "surface quasi-geostrophic (SQG) theory" by, for example, LaCasce and Mahadevan (2006) or Isern-Fontanet et al. (2008); see FW2010. The simplest interpretation of energy in Fig. 5 distant from the flat-bottom modal curves and the nondispersive line is that it is a linear response to atmospheric forcing, but a considerable literature would insist that it is the result of turbulent cascades. Presumably all mechanisms are operating to a degree. As far as the mooring data are concerned, no evidence has emerged calling for vertical structures in u, v not effectively described by the first few BTT modes; therefore, relying on their completeness, SQG and other vertically trapped motions are now ignored. [A surface-trapped flow in the data can be represented perfectly by the linear, flat-bottom modes, with its presence implying a phase locking (coherence) among them, and FW2010 discuss this problem further; note that there are many moorings showing bottom intensification, likely associated with finite topographic slopes, and these are not detectable in deep water with the altimeter.] Coupling between the barotropic and first baroclinic modes with a phase amplifying the near-surface kinetic energy will reduce the abyssal kinetic energy reminiscent of the Tailleux and McWilliams (2001) topographic energy reduction mechanism. Distinguishing between these two different reasons for mode coupling will not be simple.

In Wunsch (2009), it was speculated that motions along the nondispersive line represent a phase coupling of the barotropic and first baroclinic modes, but at the moment the hypothesis has not proved testable. For present purposes, the most agnostic approach is to assert that the energy partition found from the moorings is a reasonable one, and one might write the full spectrum in the mixed fashion as

$$\Phi_3(k,s,z) = \Phi(k,s)[(5/10)F_0^2 + (4/10)F_1(z)^2 + \varepsilon], \qquad (8)$$

where the terms F_j are the barotropic and baroclinic modes normalized to unit squared integrals and ε is an error term. The coupling is being ignored because its sign and structure are poorly known. As above, geographical factors are introduced to reflect the spatial variations of Φ, and the vertical partition likely also varies with position. Equation (A1) does permit a zero-order estimate of the depth dependence of the transport variability. (If desired, a formal three-dimensional spectrum can be readily contrived using delta functions for vertical wavenumbers.)

5. Implications

a. Trends

The interest in trends primarily concerns those that are truly secular, defined above as extending over far longer intervals than the record length. In many geophysical processes, there is a strong tendency to produce extended periods of apparent but not truly secular trends (e.g., Wunsch 1999). The definition of "far longer" is intentionally vague. The reason for being so vague is the suspicion that much of the climate system, having many long time scales, exhibits a conventional memory, red-noise-like behavior out to extremely long periods.

Real records containing trends can be written as

$$y_t = F(t) + n_t,$$

where $F(t)$ is the trend and is defined here as a process indistinguishable from deterministic; n_t is referred to as "noise" but contains all of the other physics in the record and is regarded as fundamentally stochastic. Here, $F(t)$ will be assumed to generally be linear, $F(t) = a + bt$, but quadratic, cubic, or any other plausible rule can be dealt with similarly (see also the appendix). Most trends of climate interest have at least a projection on to a straight line.

Sea level provides an interesting example of some of the challenges. From very robust information in the geological record, it is clear that global mean sea level rose during the last deglaciation by about 120 m over about 18 000 yr (e.g., Bard et al. 1996; Peltier and Fairbanks 2006) for a gross secular trend of about 0.7 cm yr^{-1}. Even this trend is not truly secular because, deeper in the past, it reverses, with global mean sea level dropping as the continental glaciers built up. For present purposes, it is viewed as deterministic; however, on much longer time scales, discussions of its nature become bound up with the murky discussion of the controls on the 100 000-yr time scales of the last 800 000 yr (see Tziperman et al. 2006 for various references), and it evidently has a mixed stochastic–deterministic character.

The sea level rise curve appears to have flattened considerably during the last about 8000 yr (the late Holocene), and one is tempted to compute a new secular trend during this period. Such a computation is surely sensible; the complications arise in the calculation of its statistical significance. As Percival and Rothrock (2005) have noted forcefully, calculation of a trend over an

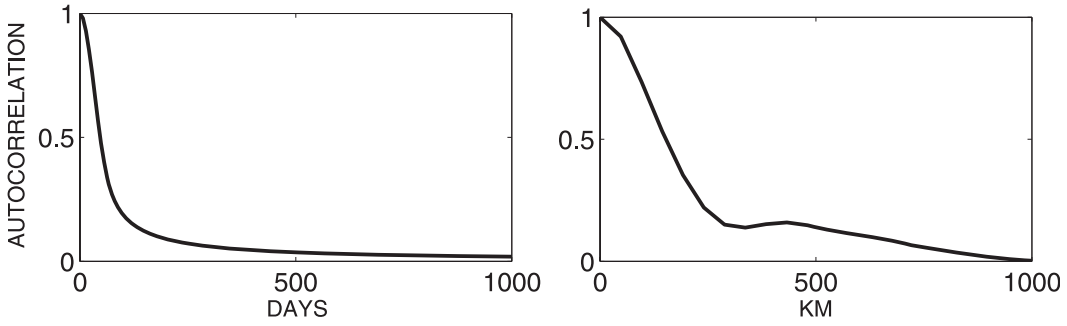

FIG. 14. The temporal (left) $R_\tau(\tau)/R_\tau(0)$ and (right) $R_\rho(\rho)/R_\rho(0)$ autocorrelations derived from the analytical frequency wavenumber spectral density.

interval chosen visually as a subregion of a much longer record produces a much more pessimistic confidence interval than does one calculated without the use of a preselected interval.

The instrumental sea level records available to us are far shorter than the time scale of the gross shift under deglaciation. High-accuracy altimetry exists, as of this writing, for only 16 yr. A number of tide gauge records (e.g., Douglas et al. 2001) extend back about 100 yr and longer, and the Brest tide gauge record has been patched together back to 1711 by Wöppelmann et al. (2008). These comparatively long records suffer, however, as do altimetric and all other long records, from the inability to fully determine trends introduced by the measurement system. Tide gauge records, depending upon location, undergo major corrections for local tectonic shifts, and often they are relocated at various times in harbors with changing configurations from construction, the technology changes, etc. Even for the modern altimetric data, there are serious concerns about drifts in corrections: Wunsch et al. (2007, appendix) and Ablain et al. (2009) describe an incomplete list of the altimetric corrections susceptible to unknown trends.

In addition to sea level and the associated heat and freshwater contributions, the other source of public agitation has been the inference of trends in oceanic volume or mass transports and (usually only implicitly) the associated enthalpy transports. The physics, and hence the statistics, of transport fluctuations and of sea level change are quite distinct, albeit not independent, with a relationship through the pressure field.

In any region, the statistical significance of a trend law will be determined in large part by the spectrum of the background variability. As discussed in textbooks (e.g., Wunsch 2006, p. 133+), the most straightforward estimate will involve using the space–time covariance $R(\tau, \rho)$, which through the generalized Wiener–Khinchin theorem (see Vanmarcke 1983) is the double Fourier transform of the spectrum,

$$R(\tau, \rho) = \int^{\infty} \int_{-\infty} \exp(2\pi i s\tau + 2\pi i k\rho)\Phi(s, k)\, ds\, dk. \quad (9)$$

Here, τ and ρ are the temporal and spatial separations between two points in a region small enough that Φ is representative of both. A full interpretation of R and the actual calculation of large-scale trends and their significance would take us far beyond the intended scope of this paper. However, as an indicator of how Φ and hence R can be used, Fig. 14 displays the two one-dimensional integrals $R_\tau(\tau)$ and $R_\rho(\rho)$ of $R(\tau, \rho)$ in which the spatial and temporal separations, respectively, have been integrated out. They have been normalized to 1 at the origin so that they are autocorrelations [e.g., $R_\tau/R(0)$ is the conventional temporal autocorrelation at one point]. Thus, integrating over all wavenumbers, two measurements at one point will effectively be decorrelated after about 200 days temporal separation, and two measurements at one time will be spatially decorrelated when separated by about 1000 km when accounting for the variability out to 16 yr.

When trends are computed over particular areas, one would account for spatial averages by integrating appropriately over $R(\tau, \rho)$ and accounting for the scale factor $A(\theta, \lambda)$. Application in this way is postponed to a later paper.

b. *Other applications*

Many applications of an analytical spectrum exist. For example, Wunsch (2008) calculated the loss of coherence in zonally separated measurements and Wunsch (2009) discussed the remarkably rapid meridional loss of coherence of the transports (which involves the meridional spectral density not dealt with here).

6. Discussion

The problem of trend determination in the ocean circulation motivates an attempt to formulate a useful

frequency–wavenumber representation of the background oceanic variability. That goal in turn leads to a long list of physics puzzles. An empirical analytical form is proposed for the zonal wavenumber and frequency content of surface pressure (elevation) variability in the subtropics. Unlike a previous model of ZW2001, it is heavily asymmetric in the eastward- and westward-going phase velocities, with much of the energy lying along the sharply defined nondispersive line, whose slope is a function of latitude, approximately βR_d^2. About 20% of the energy is eastward going. A speculative form of the spectral behavior for periods beyond the current length of the altimetric records (16 yr) is proposed.

Within the observed time scales, the proposed analytical expression seems typical of subtropical latitudes, but it clearly fails in the Southern Ocean and elsewhere, although these failures are not described here. Because the cutoff frequency for baroclinic Rossby waves rapidly diminishes with β and hence with latitude, even 15 yr of data proves short for discussing high-latitude behavior. Theoretical explanations of the frequency structures observed are not readily available, because turbulence (and unequilibrated instability) theories do not normally address the time-domain structure seen at midlatitudes. There is thus a mismatch of observational capability, which finds frequency spectra easiest to estimate, and the theoretical constructs, which are simplest in wavenumber or directed at transient behavior.

Several physical theories address rapidly propagating Rossby waves producing narrow bands in frequency–wavenumber space, and several other theories are directed at turbulent interactions producing broadband characters in that space. No comprehensive theory exists that describes either the numerical or analytical spectral versions in Figs. 5–7 or 10, although various theories predict, for example, breakup of waves into unstable modes and hence turbulence (Isachsen et al. 2007) or formation of waves from the turbulence at the Rhines scale, etc. Much of the theoretical uncertainty, only sketched here, could be reduced by better understanding of (i) the modal partition of the motions and (ii) the degree of phase locking among the modes, which could be better explored with existing data.

The parameter called U, which is supposed to represent, alternatively, a Taylor-hypothesis large-scale mean advection velocity or an RMS of the energy containing eddies, is best denoted $\tilde{U}$; it will be a sample value and itself a stochastic variable. Except in special places like the Antarctic Circumpolar Current, its value and sign would be expected to vary considerably from one realization of duration T to another. Discussions of the sampling statistics of U as a function of duration and area do not seem to be available. Whether the sharpness, overall stability, and latitude dependence of the nondispersive line are consistent with fluctuations in the sampled U is unknown.

Baroclinic instability will populate the ocean with low mode energy, and turbulent cascade arguments (going back at least to Charney 1971) will redistribute that energy in both wavenumber and vertical mode space (see, e.g., Fu and Flierl 1980; Vallis 2006; Scott and Arbic 2007; and others). Cascades of energy can take place either upscale or downscale in wavenumber and in transfers, for example, to and from barotropic mode and first and higher baroclinic modes.

What are the implications of these results for determining trends? Mathematically, the behavior of the spectrum in the low-frequency limit, $s \rightarrow 0$, is crucial because it determines whether the autocovariance decays exponentially, as with conventional random processes, or algebraically as in so-called long memory processes in which the behavior of the spectrum is that of a power law to arbitrarily long time scales. In practice, the limiting case is inaccessible from observation and not likely even physically meaningful. What are accessible are estimates of the spectral behavior for small $s > 0$, limited by record lengths. Because the presence of a trend influences that behavior, the spectral density estimates obtained here are ambiguous, ranging from purely white to weakly red and dependent upon precisely how the estimate is made. No specific evidence exists for any more exotic behavior involving so-called long memory processes, given the very long, conventional time scales present in the ocean circulation.

Altimetric data, now of order 16+ yr duration, show that considerable structure exists in the frequency–wavenumber domain for small s and that the frequency spectrum $\Phi_s(s)$, obtained by integrating out the wavenumber spectrum, will be a function of (at least) latitude. Thus, the statistical significance of any particular observed trend (a subject not explored here) will depend directly upon the geography and areal extent of the region under consideration. In particular, attaching significance levels to putative global average trends requires integration over the spatially varying structures in the background variability. Treating that background variability as geographically homogeneous can lead to incorrect conclusions about significance.

Acknowledgments. This work was supported in part by the National Aeronautics and Space Administration through JPL Jason Grant NNX08AR33G. I had useful discussions with B. Owens, C. Wortham, and R. Ferrari,

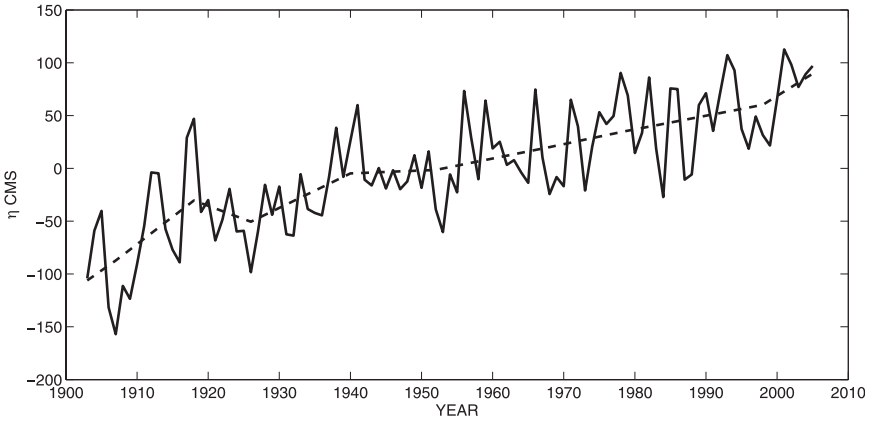

FIG. A1. Piecewise linear fit (in a 2 norm) to the 2-yr running mean Honolulu tide gauge record such that the 1 norm of the straight lines is a minimum.

and some of the anonymous reviewers' comments led to significant improvements.

APPENDIX

Piecewise Linear Trends

The assumption that the sea level is best represented as a straight-line trend plus a stochastic background is not easy to test. As one generalization, the best fit of a minimal number of linear segments produces a useful alternative representation. Here we use the "ℓ_1 trend filtering" method of Kim et al. (2009), which is based on minimizing the cost function

$$J = \|\eta(t) - f(t)\|_2 + \alpha^2 \|Df(t)\|_1, \qquad \text{(A1)}$$

where $f(t)$ is a set of continuous line segments, D is an operator computing the numerical second derivatives, and α^2 is an empirical trade-off parameter. Note that the straight-lines fit $\eta(t)$ is a least squares sense (2 norm), but the numerical second derivatives are measured in a 1-norm (absolute value) sense. See Kim et al. (2009) for a discussion of the rationale for this choice. Figure A1 shows the result, for the Honolulu tide gauge record, of choosing the value of α^2 giving the smallest 1 norm for $f(t)$. Whether this result is a more useful one than the simple fit above to the entire record is debatable. That a single simple trend does not describe such a complex phenomenon as sea level change is, however, unsurprising. The nature of the estimated low-frequency spectrum as $s \to 0$ is sensitive to the number of separate line segments that might be subtracted from records such as this one or alternatively as it would be if no trend is subtracted, and the number of pieces are treated as though part of the fractionally observed low frequencies.

REFERENCES

Ablain, M., A. Cazenave, G. Valladeau, and S. Guinehut, 2009: A new assessment of the error budget of global mean sea level rate estimated by satellite altimetry over 1993–2008. *Ocean Sci.,* **5,** 193–201.

Arbic, B. K., and W. B. Owens, 2001: Climatic warming of Atlantic intermediate waters. *J. Climate,* **14,** 4091–4108.

Bard, E., B. Hamelin, M. Arnold, L. Montaggioni, G. Cabioch, G. Faure, and F. Rougerie, 1996: Deglacial sea-level record from Tahiti corals and the timing of global meltwater discharge. *Nature,* **382,** 241–244.

Beran, J., 1994: *Statistics for Long Memory Processes*. Chapman and Hall, 315 pp.

Bindoff, N. L., and Coauthors, 2007: Observations: Oceanic climate change and sea level. *Climate Change 2007: The Physical Science Basis,* S. Solomon et al., Eds., Cambridge University Press, 385–432.

Bryden, H. L., E. L. McDonagh, and B. A. King, 2003: Changes in ocean water mass properties: Oscillations or trends? *Science,* **300,** 2086–2088.

Cazenave, A., and R. S. Nerem, 2004: Present-day sea level change: Observations and causes. *Rev. Geophys.,* **42,** RG3001, doi:10.1029/2003RG000139.

Charney, J. G., 1971: Geostrophic turbulence. *J. Atmos. Sci.,* **28,** 1087–1095.

Chelton, D. B., and M. G. Schlax, 1996: Global observations of oceanic Rossby waves. *Science,* **272,** 234–238.

——, R. A. DeSzoeke, M. G. Schlax, K. El Naggar, and N. Siwertz, 1998: Geographical variability of the first baroclinic Rossby radius of deformation. *J. Phys. Oceanogr.,* **28,** 433–460.

——, M. G. Schlax, R. M. Samelson, and R. A. de Szoeke, 2007: Global observations of large oceanic eddies. *Geophys. Res. Lett.,* **34,** L15606, doi:10.1029/2007GL030812.

Colosi, J. A., and W. Munk, 2006: Tales of the venerable Honolulu tide gauge. *J. Phys. Oceanogr.,* **36,** 967–996.

Douglas, B. C., M. S. Kearney, and S. R. Leatherman, Eds., 2001: *Sea Level Rise, History and Consequences*. Academic Press, 228 pp.

Ferrari, R., and C. Wunsch, 2009: Ocean circulation kinetic energy: Reservoirs, sources, and sinks. *Annu. Rev. Fluid Mech.,* **41,** 253–282.

——, and ——, 2010: The distribution of eddy kinetic and potential energies in the global ocean. *Tellus,* **62A,** 92–108.

Frankignoul, C., P. Muller, and E. Zorita, 1997: A simple model of the decadal response of the ocean to stochastic wind forcing. *J. Phys. Oceanogr.,* **27,** 1533–1546.

——, A. Czaja, and B. L'Heveder, 1998: Air–sea feedback in the North Atlantic and surface boundary conditions for ocean models. *J. Climate,* **11,** 2310–2324.

Fu, L.-L., and G. R. Flierl, 1980: Non-linear energy and enstrophy transfers in a realistically stratified ocean. *Dyn. Atmos. Oceans,* **4,** 219–246.

——, and A. Cazenave, 2000: *Satellite Altimetry and Earth Sciences: A Handbook of Techniques and Applications*. Academic Press, 463 pp.

Garrett, C., and W. Munk, 1972: Space-time scales of internal waves. *Geophys. Astrophys. Fluid Dyn.,* **3,** 225–264.

Glazman, R. E., and P. B. Weichman, 2005: Meridional component of oceanic Rossby wave propagation. *Dyn. Atmos. Oceans,* **38,** 173–193.

Hinze, J. O., 1975: *Turbulence*. 2nd ed. McGraw-Hill, 790 pp.

Huybers, P., and W. Curry, 2006: Links between annual, Milankovitch and continuum temperature variability. *Nature,* **441,** 329–332.

Isachsen, P. E., J. H. LaCasce, and J. Pedlosky, 2007: Rossby wave instability and apparent phase speeds in large ocean basins. *J. Phys. Oceanogr.,* **37,** 1177–1191.

Isern-Fontanet, J., G. Lapeyre, P. Klein, B. Chapron, and M. W. Hecht, 2008: Three-dimensional reconstruction of oceanic mesoscale currents from surface information. *J. Geophys. Res.,* **113,** C09005, doi:10.1029/2007JC004692.

Johnson, G. C., S. Mecking, B. M. Sloyan, and S. E. Wijffels, 2007: Recent bottom water warming in the Pacific Ocean. *J. Climate,* **20,** 5365–5375.

Joyce, T. M., R. S. Pickart, and R. C. Millard, 1999: Long-term hydrographic changes at 52 and 66°W in the North Atlantic subtropical gyre & Caribbean. *Deep-Sea Res. I,* **46,** 245–278.

Katz, E. J., 1975: Tow spectra from MODE. *J. Geophys. Res.,* **80,** 1163–1167.

Killworth, P. D., and J. R. Blundell, 2003a: Long extratropical planetary wave propagation in the presence of slowly varying mean flow and bottom topography. Part I: The local problem. *J. Phys. Oceanogr.,* **33,** 784–801.

——, and ——, 2003b: Long extratropical planetary wave propagation in the presence of slowly varying mean flow and bottom topography. Part II: Ray propagation and comparison with observations. *J. Phys. Oceanogr.,* **33,** 802–821.

Kim, S.-J., K. Koh, S. Boyd, and D. Gorinevsky, 2009: l_1 trend filtering. *SIAM Rev.,* **51,** 339–360.

Kutzbach, J. E., 1978: Nature of climate and climatic variations. *IEEE Trans. Geosci. Remote Sens.,* **16,** 23–29.

LaCasce, J. H., and A. Mahadevan, 2006: Estimating subsurface horizontal and vertical velocities from sea-surface temperature. *J. Mar. Res.,* **64,** 695–721.

Le Traon, P. Y., F. Nadal, and N. Ducet, 1998: An improved mapping method of multisatellite altimeter data. *J. Atmos. Oceanic Technol.,* **15,** 522–534.

Longuet-Higgins, M. S., 1965: Planetary waves on a rotating sphere. II. *Proc. Roy. Soc. London,* **284A,** 40–68.

Maharaj, A. M., P. Cipollini, N. J. Holbrook, P. D. Killworth, and J. R. Blundell, 2007: An evaluation of the classical and extended Rossby wave theories in explaining spectral estimates of the first few baroclinic modes in the South Pacific Ocean. *Ocean Dyn.,* **57,** 173–187.

Maximenko, N. A., O. V. Melnichenko, P. P. Niiler, and H. Sasaki, 2008: Stationary mesoscale jet-like features in the ocean. *Geophys. Res. Lett.,* **35,** L08603, doi:10.1029/2008GL033267.

Mazloff, M. R., P. Heimbach, and C. Wunsch, 2010: An eddy-permitting Southern Ocean state estimate. *J. Phys. Oceanogr.,* **40,** 880–899.

McCoy, E. J., A. T. Walden, and D. B. Percival, 1998: Multitaper spectral estimation of power law processes. *IEEE Trans. Signal Process.,* **46,** 655–668.

Mitchell, J. M., 1976: Overview of variability and its causal mechanisms. *Quat. Res.,* **6,** 481–493.

Overland, J. E., D. B. Percival, and H. O. Mofjeld, 2006: Regime shifts and red noise in the North Pacific. *Deep-Sea Res.,* **53,** 582–588.

Peltier, W. R., and R. G. Fairbanks, 2006: Global glacial ice volume and Last Glacial Maximum duration from an extended Barbados sea level record. *Quat. Sci. Rev.,* **25,** 3322–3337.

Percival, D. B., and A. T. Walden, 1993: *Spectral Analysis for Physical Applications: Multitaper and Conventional Univariate Techniques*. Cambridge University Press, 583 pp.

——, and D. A. Rothrock, 2005: ''Eyeballing'' trends in climate time series: A cautionary note. *J. Climate,* **18,** 886–891.

Philander, S. G. H., 1978: Forced oceanic waves. *Rev. Geophys.,* **16,** 15–46.

Polyakov, I. V., U. S. Bhatt, H. L. Simmons, D. Walsh, J. E. Walsh, and X. Zhang, 2005: Multidecadal variability of North Atlantic temperature and salinity during the twentieth century. *J. Climate,* **18,** 4562–4581.

Rhines, P. B., 1977: The dynamics of unsteady currents. *The Sea,* E. D. Goldberg, Ed., *Marine Chemistry,* Vol. 6, 189–318.

Roemmich, D., and C. Wunsch, 1984: Apparent changes in the climatic state of the deep North Atlantic Ocean. *Nature,* **307,** 447–450.

Scott, R. B., and B. K. Arbic, 2007: Spectral energy fluxes in geostrophic turbulence: Implications for ocean energetics. *J. Phys. Oceanogr.,* **37,** 673–688.

Smith, R. L., 1993: Long-range dependence and global warming. *Statistics for the Environment,* V. Barnett and K. F. Turkman, Eds., Wiley, 141–161.

Sturges, W., and B. G. Hong, 1995: Wind forcing of the Atlantic thermocline along 32°N at low frequencies. *J. Phys. Oceanogr.,* **25,** 1706–1715.

——, ——, and A. J. Clarke, 1998: Decadal wind forcing of the North Atlantic subtropical gyre. *J. Phys. Oceanogr.,* **28,** 659–668.

Tailleux, R., and J. C. McWilliams, 2001: The effect of bottom pressure decoupling on the speed of extratropical, baroclinic Rossby waves. *J. Phys. Oceanogr.,* **31,** 1461–1476.

Tulloch, R., J. Marshall, and K. S. Smith, 2009: Interpretation of the propagation of surface altimetric observations in terms of planetary waves and geostrophic turbulence. *J. Geophys. Res.,* **114,** C02005, doi:10.1029/2008JC005055.

Tziperman, E., M. E. Raymo, P. Huybers, and C. Wunsch, 2006: Consequences of pacing the Pleistocene 100 kyr ice ages by nonlinear phase locking to Milankovitch forcing. *Paleoceanography,* **21,** PA4206, doi:10.1029/2005PA001241.

Vallis, G., 2006: *Atmospheric and Oceanic Fluid Dynamics*. Cambridge University Press, 745 pp.

Vanmarcke, E., 1983: *Random Fields Analysis and Synthesis*. MIT Press, 382 pp.

Vinogradov, S. V., R. M. Ponte, P. Heimbach, and C. Wunsch, 2008: The mean seasonal cycle in sea level estimated from a data-constrained general circulation model. *J. Geophys. Res.,* **113,** C03032, doi:10.1029/2007JC004496.

Vyushin, D. I., and P. J. Kushner, 2009: Power-law and long-memory characteristics of the atmospheric general circulation. *J. Climate,* **22,** 2890–2904.

Wöppelmann, G., N. Pouvreau, A. Coulomb, B. Simon, and P. L. Woodworth, 2008: Tide gauge datum continuity at Brest since 1711: France's longest sea-level record. *Geophys. Res. Lett.,* **35,** L22605, doi:10.1029/2008GL035783.

Wunsch, C., 1997: The vertical partition of oceanic horizontal kinetic energy. *J. Phys. Oceanogr.,* **27,** 1770–1794.

——, 1999: The interpretation of short climate records, with comments on the North Atlantic and Southern Oscillations. *Bull. Amer. Meteor. Soc.,* **80,** 245–255.

——, 2006: *Discrete Inverse and State Estimation Problems: With Geophysical Fluid Applications*. Cambridge University Press, 371 pp.

——, 2008: Mass and volume transport variability in an eddy-filled ocean. *Nat. Geosci.,* **1,** 165–168.

——, 2009: The oceanic variability spectrum and transport trends. *Atmos.–Ocean,* **47,** 281–291.

——, and P. Heimbach, 2007: Practical global oceanic state estimation. *Physica D,* **230,** 197–208.

——, and ——, 2009: The global zonally integrated ocean circulation, 1992–2006: Seasonal and decadal variability. *J. Phys. Oceanogr.,* **39,** 351–368.

——, R. M. Ponte, and P. Heimbach, 2007: Decadal trends in sea level patterns: 1993–2004. *J. Climate,* **20,** 5889–5911.

Zang, X. Y., and C. Wunsch, 1999: The observed dispersion relationship for North Pacific Rossby wave motions. *J. Phys. Oceanogr.,* **29,** 2183–2190.

——, and ——, 2001: Spectral description of low-frequency oceanic variability. *J. Phys. Oceanogr.,* **31,** 3073–3095.